Subnormothermic *ex vivo* lung perfusion possibly protects against ischemia-reperfusion injury via the mTORC-HIF-1α pathway

Jee Won Suh[1], Soo Jin Park[2], Young Wha Koh[3], Daun Seo[2], Seokjin Haam[2]

[1]Department of Thoracic and Cardiovascular Surgery, Yongin Severance Hospital, Yonsei University College of Medicine, Yongin, Gyeonggi-do, Republic of Korea; [2]Department of Thoracic and Cardiovascular Surgery, Ajou University Hospital, Ajou University School of Medicine, Suwon, Republic of Korea; [3]Department of Pathology, Ajou University Hospital, Ajou University School of Medicine, Suwon, Republic of Korea

Contributions: (I) Conception and design: JW Suh, S Haam; (II) Administrative support: S Haam; (III) Provision of study materials or patients: S Haam; (IV) Collection and assembly of data: SJ Park, YW Koh, D Seo, S Haam; (V) Data analysis and interpretation: JW Suh, SJ Park, S Haam; (VI) Manuscript writing: All authors; (VII) Final approval of manuscript: All authors.

Correspondence to: Seokjin Haam, MD, PhD. Department of Thoracic and Cardiovascular Surgery, Ajou University Hospital, Ajou University School of Medicine, 164 World cup-ro, Yeongtong-gu, Suwon 16499, Republic of Korea. Email: haamsj@aumc.ac.kr.

Background: Ex vivo lung perfusion (EVLP) is a useful technique for evaluating and repairing donor lungs for transplantation. However, studies examining the effects of perfusate temperature on graft function are limited. Thus, this study aimed to examine these effects during EVLP on ischemic-reperfusion injury in the donor lung.

Methods: Twenty-four male Sprague-Dawley rats were randomly divided into three groups, as follows: no treatment (sham group, n=5), normothermic EVLP (37 ℃, n=5), and subnormothermic EVLP (30 ℃, n=5). Lung function analyses, including oxygen capacity (OC), compliance, and pulmonary vascular resistance (PVR), were performed hourly during EVLP. Further, after 4 h of EVLP, histological evaluation of the right lobe was performed using the lung injury severity (LIS) scale. The expression levels of inflammatory cytokines such as tumor necrosis factor (TNF)-α, interleukin (IL)-1β, IL-6, and IL-18 were evaluated. Metabolomic analysis of left lung tissues was conducted using capillary electrophoresis time-of-flight mass spectrometry (CE-TOFMS) after 4 h of EVLP in the EVLP groups and after 1 h of cold preservation in the sham group.

Results: Compared with those in the normothermic group, in the subnormothermic group, functional parameters during EVLP and subsequent histologic results were significantly superior, expression levels of inflammatory cytokines such as TNF-α, IL-1β, IL-6, and IL-18 were significantly lower, and glycolytic activity was significantly decreased. Furthermore, expression levels of mammalian target of rapamycin complex (mTORC), hypoxia-inducible factor (HIF) 1α, and nucleotide-binding domain, leucine-rich-containing family pyrin domain containing 3 (NLRP3) and its effector caspase-1 were significantly lower in the subnormothermic group than in the normothermic group.

Conclusions: EVLP with subnormothermic perfusion improves lung graft function by reducing the expression of pro-inflammatory cytokines and glycolytic activity during EVLP. Additionally, EVLP can be a useful target for the improvement of graft function after transplantation.

Keywords: Ex vivo lung perfusion (EVLP); ischemia-reperfusion injury (IR injury); graft function

Introduction

Lung transplantation is the only curative treatment for patients with end-stage lung disease. Due to the low procurement rate associated with the limited availability of lungs from brain death donors, only 15–25% of potential donor lungs are successfully transplanted (1). This low rate is attributed to aspiration-associated injuries, barotraumas, and ventilator-associated pneumonia during brain death (2). Considering increased waiting-list mortalities due to the low procurement rate, alternative options involving marginal and circulatory death donors have emerged. Ex vivo lung perfusion (EVLP) is a method to increase lung utility rates and reduce graft dysfunction due to ischemia-reperfusion (IR) injuries.

EVLP is a well-known method to evaluate and preserve organ function when donors do not meet standard donor criteria. Currently, clinically available EVLP protocols (from the Lund, Toronto, and Organ Care System) are mainly used under normothermic conditions (37 ℃) (3). To mimic physiological conditions, the lung is perfused and ventilated *ex vivo* at body temperature (4). Until recently, EVLP was performed under normothermic or near normothermic conditions because hypothermia can reduce metabolic function which in turn makes it impossible to accurately evaluate organ function and recovery (5). Although normothermic EVLP increases waste and pro-inflammatory cytokine production (6-8), it is considered safe and reliable for the repair of damaged donor organs (9-11), thereby enhancing the function of marginal donor lungs and improving post-transplant outcomes (4,12-15).

Few studies have examined the effects of EVLP perfusate temperature on donor lung function, but recent studies observed the effects of perfusate temperature on EVLP in lung transplants. Subnormothermic EVLP shows significantly lower energy consumption and induces reduced inflammatory response compared with normothermic EVLP, and these protective effects persist in rat models of lung donation after circulatory death (6-8,16).

Metabolomic analysis may provide important information about the extent of tissue damage or repair (17). This analysis quantitatively assesses dynamic responses to physiological and pathological changes (18). As a consequence of low perfusate temperature, oxidative stress and alterations in specific energy metabolites emerge (17,19,20), serving as indicators for monitoring organ function and evaluating perfusion injury in organ transplants (17). Additionally, hypoxia-inducible factor 1α (HIF-1α) is involved in these metabolic changes, especially in glucose metabolism, and it is related to inflammatory pathways in the lung (21).

Objective

This study aimed to investigate the mechanisms by which subnormothermic perfusate during EVLP is associated with a protective effect against IR injuries in a rat EVLP model. Furthermore, the study investigated changes in lung grafts after subnormothermic and normothermic EVLP, focusing on energy metabolism and inflammatory pathways. The key study design and question were prepared before the study, but the protocol was not registered. We present this article in accordance with the ARRIVE reporting checklist (available at https://jtd.amegroups.com/article/view/10.21037/jtd-23-1809/rc).

Methods

Animals

Male Sprague-Dawley rats (DBL, Eumseong, Korea) weighing 280–320 g were used in this study. All experimental and animal care procedures were conducted in accordance with the Laboratory Animal Welfare Act, the Guide for the Care and Use of Laboratory Animals provided by the Ajou University Institutional Animal Care and Use Committee (IACUC) (No. 2016-0047), and the Guide for the Care and Use of Laboratory Animals (NIH


Highlight box

Key findings

• Subnormothermic ex vivo lung perfusion (EVLP) was associated with a significantly lower expression of inflammatory cytokines and mammalian target of rapamycin complex, hypoxia-inducible factor 1α, and nucleotide-binding domain, leucine-rich-containing family pyrin domain containing 3 compared to normothermic EVLP.

What is known and what is new?

• In previous studies, subnormothermic EVLP exhibited favorable outcomes in rats in comparison to normothermic EVLP.

• Compared to the subnormothermic EVLP group, the normothermic EVLP group predominantly used glycolysis for energy metabolism.

What is the implication, and what should change now?

• Subnormothermic perfusion improves lung graft function during EVLP through this energy metabolism switch.
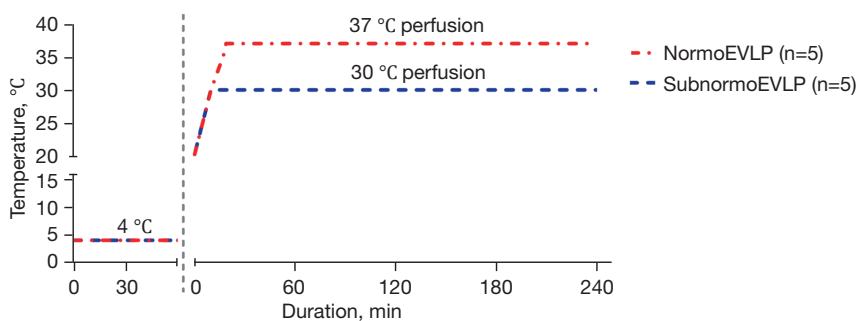
Figure 1 Protocol for EVLP. The lung grafts are preserved at 4 ℃ for 1 h. Thereafter, sham group samples are preserved at 4 ℃, whereas EVLP is applied to the normoEVLP and subnormoEVLP groups for 4 h at 37 ℃ or 30 ℃, respectively. EVLP, ex vivo lung perfusion; qPCR, quantitative polymerase chain reaction.

Publication No. 86-23, revised 1996).

Experimental animal protocol for EVLP

Fifteen rats were randomly assigned using a computer-based random order generator to one of the following groups: no treatment (sham group, n=5), normothermic (37 ℃) EVLP (normoEVLP, n=5), and subnormothermic (30 ℃) EVLP (subnormoEVLP, n=5). We selected a small sample size because this experiment would produce homogeneous results during repeated execution. For each experiment, one rat from the same cage and the same breeding environment was assigned to each group. The basic anesthesia and EVLP procedures were performed according to a previously published protocol (see Appendix 1) (22,23). In the sham group, lung grafts were preserved at 4 ℃ for 1 h after harvesting. In the normoEVLP group, the perfusate temperature was gradually increased to 37 ℃ for 20 min and maintained at 37 ℃ for the entire EVLP period. In the subnormoEVLP group, the perfusate temperature was increased to 30 ℃ for 10 min and maintained at 30 ℃ throughout the EVLP period (*Figure 1*). Due to the experimental process, blinding of pulmonary function tests was not possible; however, double-blinded histology, quantitative reverse transcription-polymerase chain reaction

(qRT-PCR), and metabolic analysis were performed.

Evaluation of pulmonary function during EVLP

Lung function parameters were measured hourly during EVLP. Mechanical ventilation was performed with a fraction of inspired oxygen (FiO_2) of 1.0 for 10 min before each measurement. Functional parameters were measured, including oxygen capacity {OC, calculated as [left atrial (LA) perfusate PO_2 – pulmonary arterial (PA) perfusate PO_2]/FiO_2 through arterial blood gas analysis}, pulmonary vascular resistance [PVR, calculated as (PA pressure – LA pressure) × 80/PA flow], and dynamic lung compliance {tidal volume (TV)/[peak airway pressure – peak end expiratory pressure (PEEP)]}.

Histopathological evaluation of lung tissue

After 4 h of EVLP, the upper right lobes of the lungs were fixed with 10% buffered formalin and stained with hematoxylin and eosin. These histopathological samples were analyzed by a blinded pathologist using the modified lung injury severity (LIS) scale (24) based on a 5-point (0–4) scale separately assessing (I) alveolar capillary congestion; (II) hemorrhage; (III) infiltration/aggregation of neutrophils

in the airspace or vessel wall; and (IV) thickness of alveolar wall/hyaline membrane formation. The LIS score was calculated as the sum of subscores.

RNA extraction and qRT-PCR

qRT-PCR was performed to evaluate the gene expression levels of inflammatory cytokines and enzymes associated with the glycolysis pathway along with those of mammalian target of rapamycin complex (mTORC), HIF-1α, and nucleotide-binding domain, leucine-rich-containing family pyrin domain containing 3 (NLRP3). RNA was extracted from the left lung after 1 h of cold preservation in the sham group and after 4 h of EVLP in the EVLP groups. Total RNA was isolated from the upper left lung lobes using TRIzol reagent (#TR118, Molecular Research Center Inc., Cincinnati, OH, USA) according to the manufacturer's protocol. For qRT-PCR, 1 µg RNA was reverse transcribed using AMV Reverse Transcriptase (#M0277L, New England Biolabs, Ipswich, MA, USA). Transcript levels of target genes were quantified with 2× KAPA SYBR Fast qPCR Master Mix (#kk4602, Kapa Biosystems, Cape Town, South Africa) using the StepOnePlus™ Real-Time PCR System 510 (Applied Biosystems, Foster City, CA, USA). For each target gene, the transcript level was normalized to that of glyceraldehyde 3-phosphate dehydrogenase and calculated using the standard ΔΔCT method. The primer sequences are shown in Table S1.

Metabolic profiling by capillary electrophoresis time-of-flight mass spectrometry (CE-TOFMS)

For metabolic profiling, isolated RNA samples were sent to Human Metabolome Technologies (HMT), Inc. (Yamagata, Japan). CE-TOFMS was performed using an Agilent CE Capillary Electrophoresis System (Agilent Technologies Inc., Waldbronn, Germany). Details of sample preparation and CE-TOFMS conditions are described in the Appendix 1.

Peaks detected in the CE-TOFMS analysis were extracted using automatic integration software (MasterHands ver. 2.19.0.2, Keio University, Tokyo, Japan), and the extracted data included m/z, migration time (MT), and peak area. Five lung samples from each experimental group were used for metabolomic analysis, and 292 peaks (175 in cation and 117 in anion mode) were detected. The peak area was converted to the relative peak area using a previously published equation (25). Putative metabolites were assigned from the HMT standard library and known-unknown peak library based on m/z (tolerance ±10 ppm[3]) and MT (tolerance ±0.5 min). Among the target metabolites, 88 (50 in cation and 38 in anion mode) were detected and quantified. Hierarchical cluster analysis and principal component analysis (PCA) were performed using statistical software developed at HMT (25). The peak profiles with putative metabolites were represented on metabolic pathway maps using VANTED (Visualization and Analysis of Networks containing Experimental Data, https://www.cls.uni-konstanz.de/software/vanted/download/) software. The pathway map was prepared according to metabolic pathways known to exist in human cells. Metabolite abundance differences were considered significant at P values <0.05 for the final corrected value.

Statistical analysis

No data or experiments were excluded from the analysis. We used descriptive statistics for continuous parameters, and these were expressed as mean ± standard error of the mean. LIS scores were compared using Fisher's exact test. Lung functional parameters were statistically analyzed using two-way analysis of variance (ANOVA) with Sidak's multiple comparisons test. Gene expression and metabolite levels were statistically analyzed using one-way ANOVA with Tukey's multiple comparison test. All statistical analyses were performed using SPSS 26 (IBM Corp, Armonk, NY, USA), and figures were prepared using GraphPad Prism 9 (GraphPad Software, San Diego, CA, USA). Statistical significance was set at P<0.05.

Results

Lung function during EVLP

Functional parameters during EVLP significantly differed between the normoEVLP and subnormoEVLP groups regarding OC (1-h normoEVLP *vs.* subnormoEVLP, 302.2±17.51 *vs.* 419.4±18.76; 4-h normoEVLP *vs.* subnormoEVLP, 306.6±16.09 *vs.* 368.6±30.51, P<0.001) and PVR (1-h normoEVLP *vs.* subnormoEVLP, 0.79±0.04 *vs.* 0.69±0.05 mmHg/mL/min; 4-h normoEVLP *vs.* subnormoEVLP, 1.10±0.11 *vs.* 0.74±0.06 mmHg/mL/min, P<0.001). In contrast, lung compliance did not differ significantly (1-h normoEVLP *vs.* subnormoEVLP, 0.19±0.03 *vs.* 0.19±0.01 dyne; 4-h normoEVLP *vs.* subnormoEVLP, 0.18±0.04 *vs.* 0.18±0.02 dyne, P=0.75; *Figure 2*). During EVLP, lung function was significantly
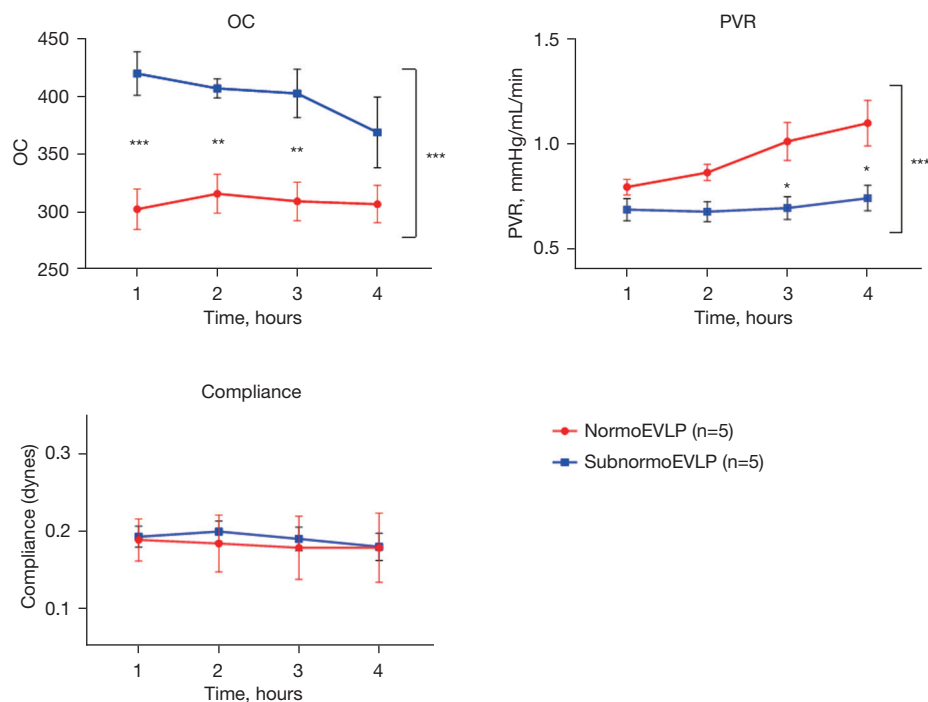
Figure 2 Analyses of EVLP parameters and lung graft pathologic findings. Functional parameters, including OC (P<0.001), PVR (P<0.001), and dynamic lung compliance (Cdyn; P=0.75), are measured every hour during EVLP. Graft function shows statistically significant superiority in terms of OC and PVR in the subnormoEVLP group compared with the normoEVLP group (*, P<0.05; **, P<0.01; ***, P<0.001, two-way analysis of variance). OC, oxygen capacity; PVR, pulmonary vascular resistance; EVLP, ex vivo lung perfusion.

superior in the subnormoEVLP group in terms of OC and PVR than in the normoEVLP group.

Histological analysis

There were significant differences in histological changes between the normoEVLP and subnormoEVLP groups (LIS scores =8.75±4.72 and 1.0±1.16, respectively; P=0.04). Alveolar wall thickening and inflammatory cell accumulation in alveolar spaces were observed in the normoEVLP group, whereas the normal alveolar structure was well maintained in the subnormoEVLP group (*Figure 3*).

Cytokine expression

The messenger RNA (mRNA) levels of tumor necrosis factor (TNF)-α (sham: 1, normoEVLP: 16.780±3.55, subnormoEVLP: 2.719±0.69; sham *vs.* normoEVLP, P<0.001; sham *vs.* subnormoEVLP, P=0.83; and normoEVLP *vs.* subnormoEVLP, P=0.001), interleukin (IL)-1β (sham: 1, normoEVLP: 24.18±7.83,

subnormoEVLP: 3.404±0.72; sham *vs.* normoEVLP, P=0.009; sham *vs.* subnormoEVLP, P=0.92; and normoEVLP *vs.* subnormoEVLP, P=0.01), IL-6 (sham: 1, normoEVLP: 19.67±2.35, subnormoEVLP: 4.978±1.65; sham *vs.* normoEVLP, P<0.001; sham *vs.* subnormoEVLP, P=0.24; and normoEVLP *vs.* subnormoEVLP, P<0.001), and IL-18 (sham: 1, normoEVLP: 12.93±4.96, subnormoEVLP: 1.807±0.22; sham *vs.* normoEVLP, P=0.03; sham *vs.* subnormoEVLP, P=0.97; and normoEVLP *vs.* subnormoEVLP, P=0.04) were significantly higher in the normoEVLP group than in the sham and subnormoEVLP groups (*Figure 4*).

Metabolite analysis

Based on the PCA results, metabolites and pathways could be classified into three groups. Metabolites related to the tricarboxylic acid (TCA) cycle and energy conversion (butyric acid, isobutyric acid, 8-hydroxyoctanoic acid, 2-hydroxyoctanoic acid, leucine, isoleucine, and valine) that showed different trends between sham and the
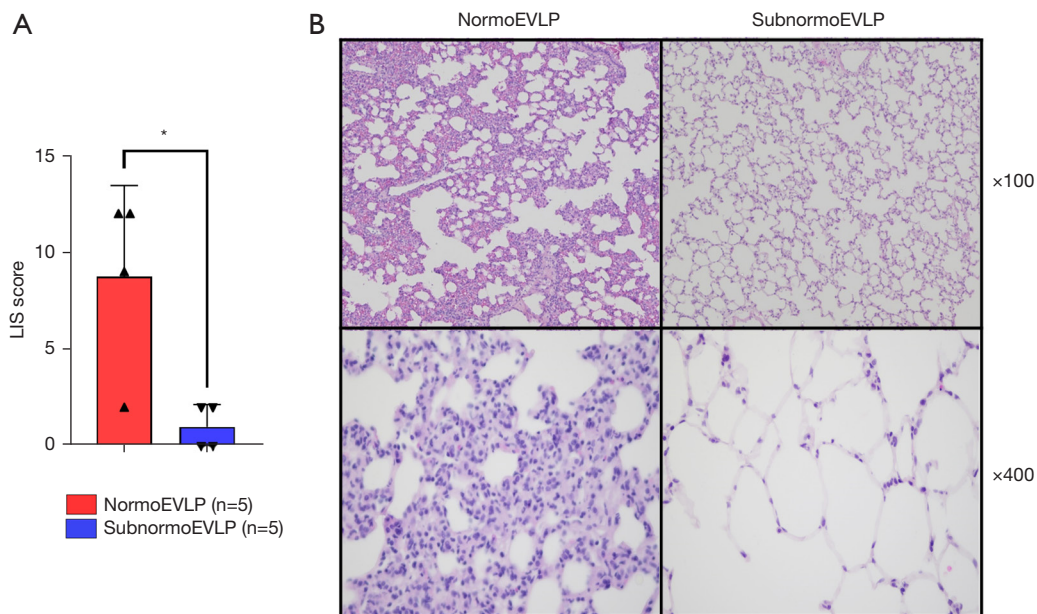
2370

Suh et al. Subnormothermic lung perfusion reduces lung injuries

Figure 3 LIS scores and histological findings in H&E-stained sections. (A) The LIS score is significantly higher in the normoEVLP group than in the subnormoEVLP group (*, P<0.05, Fisher's exact test). (B) Histologic findings in grafts (H&E, original magnifications ×100 and ×400); normoEVLP (left) and subnormoEVLP (right). Alveolar wall thickening and inflammatory cell accumulation can be observed in the normoEVLP group. The normal alveolar structure is maintained in the subnormoEVLP group. LIS, lung injury severity; EVLP, ex vivo lung perfusion; H&E, hematoxylin and eosin.

other two groups were most common (Table S2). Metabolites with different trends between the normoEVLP and subnormoEVLP groups were related to carbohydrate metabolism (UDP-N-acetylgalactosamine, UDP-N-acetylglucosamine, glucose 1-phosphate, N-acetylglucosamine 1-phosphate, phosphoenolpyruvic acid, and pyruvic acid). Thus, it was possible to identify metabolites for differentiating between the experimental groups. Details of PCA results using the detected peaks are shown in Figure S1, and the metabolites with the 10 highest and lowest PCA loading factors are listed in Table S2.

Glucose metabolism

The levels of metabolites from early glycolysis steps, such as glucose-6-phosphate (G6P) (normoEVLP vs. subnormoEVLP, 0.001765±0.000654 vs. 0.004330±0.000839; P=0.13), fructose-6-phosphate (F6P) (0.0003834±0.000128 vs. 0.0009974±0.000226; P=0.10), and fructose-1,6-bisphosphate (F1,6P) (0.001849±0.00061 vs. 0.002430±0.00030; P=0.67), indicated a tendency toward lower values in the normoEVLP group than in the subnormoEVLP group. The activity of glycolysis-related

enzymes, such as hexokinase (HK) and phosphofructokinase (PFK), was significantly higher in the normoEVLP group than in the subnormoEVLP group (normoEVLP vs. subnormoEVLP: HK, 5.879±1.999 vs. 0.2082±0.072, P=0.01; and PFK, 2.649±0.387 vs. 0.3856±0.125, P<0.001; Figure 5).

TCA cycle

The TCA cycle metabolites pyruvate, cis-aconitic acid, and α-ketoglutarate (KG) were not significantly different between the normoEVLP and subnormoEVLP groups (Figure 6). The levels of isocitric acid (sham 0.000767±0.0005, normoEVLP 0.000085±0.000085, subnormoEVLP 0.000299±0.00013; sham vs. normoEVLP, P<0.001; sham vs. subnormoEVLP, P=0.01; normoEVLP vs. subnormoEVLP, P=0.29), fumaric acid (sham 0.0019±0.00013, normoEVLP 0.00096±0.00021, subnormoEVLP 0.0012±0.000080; sham vs. normoEVLP, P=0.002; sham vs. subnormoEVLP, P=0.01; normoEVLP vs. subnormoEVLP, P=0.56), and malic acid (sham 0.0182±0.0011, normoEVLP 0.0099±0.0012, subnormoEVLP 0.1125±0.00035; sham vs. normoEVLP,
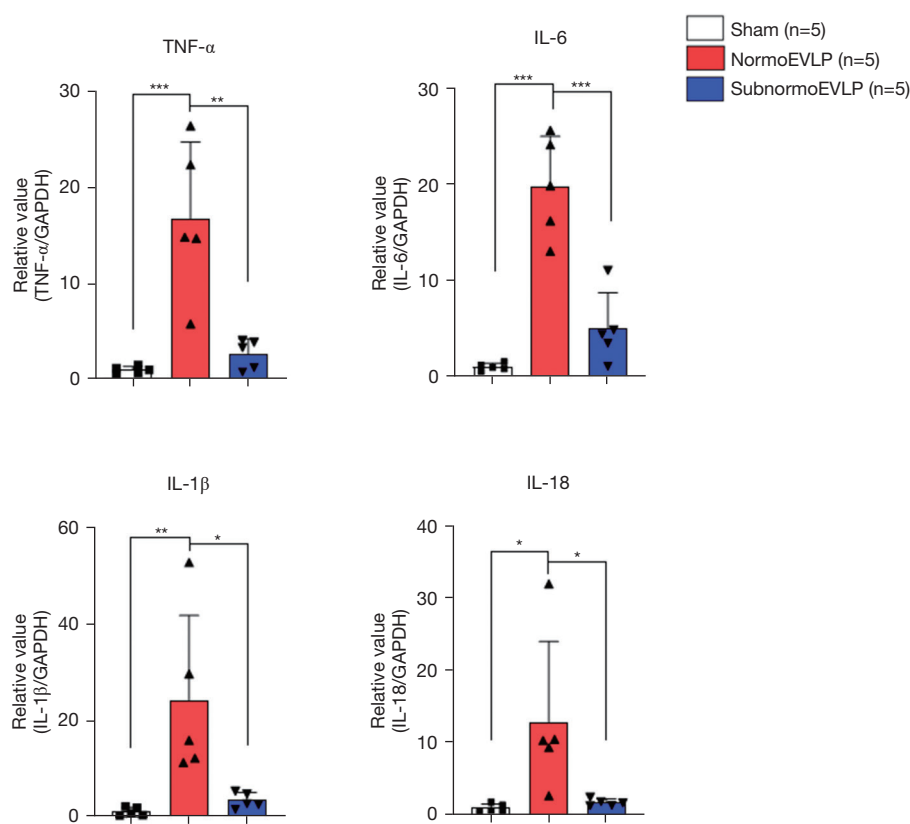
Figure 4 Pro-inflammatory cytokine mRNA levels in samples from the sham, normoEVLP, and subnormoEVLP groups (*, P<0.05; **, P<0.01; and ***, P<0.001; one-way analysis of variance). In the normoEVLP group, inflammatory cytokines are significantly upregulated compared with those in the sham group. These changes are prevented in the subnormoEVLP group, and the levels are similar to those in the sham group. TNF-α, tumor necrosis factor-α; GAPDH, glyceraldehyde 3-phosphate dehydrogenase; IL, interleukin; EVLP, ex vivo lung perfusion; mRNA, messenger RNA.

$P<0.001$; sham *vs.* subnormoEVLP, $P<0.001$; normoEVLP *vs.* subnormoEVLP, $P=0.59$) were significantly decreased in both EVLP groups compared to the sham group. There were no significant differences between the normoEVLP and subnormoEVLP groups, and they showed similar trends in both groups.

mTORC-HIF-1α-NLRP3 inflammasome pathway signaling

The mRNA expression levels of mTORC (normoEVLP *vs.* subnormoEVLP, 4.092±0.9610 *vs.* 0.2626±0.0815; $P=0.001$) and HIF-1α (5.614±1.295 *vs.* 0.1616±0.113; $P<0.001$) significantly increased in the normoEVLP group compared with those in the subnormoEVLP group. The NLRP3 level (normoEVLP *vs.* subnormoEVLP,

4.782±1.004 *vs.* 2.309±0.597; $P=0.05$) tended to be higher in the normoEVLP group than in the subnormoEVLP group without reaching statistical significance, but its main effector caspase-1 (normoEVLP *vs.* subnormoEVLP, 2.798±0.471 *vs.* 0.3470±0.115; $P<0.001$) had significantly higher levels in the normoEVLP group (*Figure 7*).

Discussion

The concept of using EVLP to enhance the rate of organ utilization has gained widespread acceptance primarily due to the persistent shortage of donor organs. Some studies reported that normothermic EVLP maintains stable donor graft function and induces minimal injuries (4,26). Although a few recent studies have demonstrated the utility of subnormothermic EVLP (7,8,16), the perfusate temperature
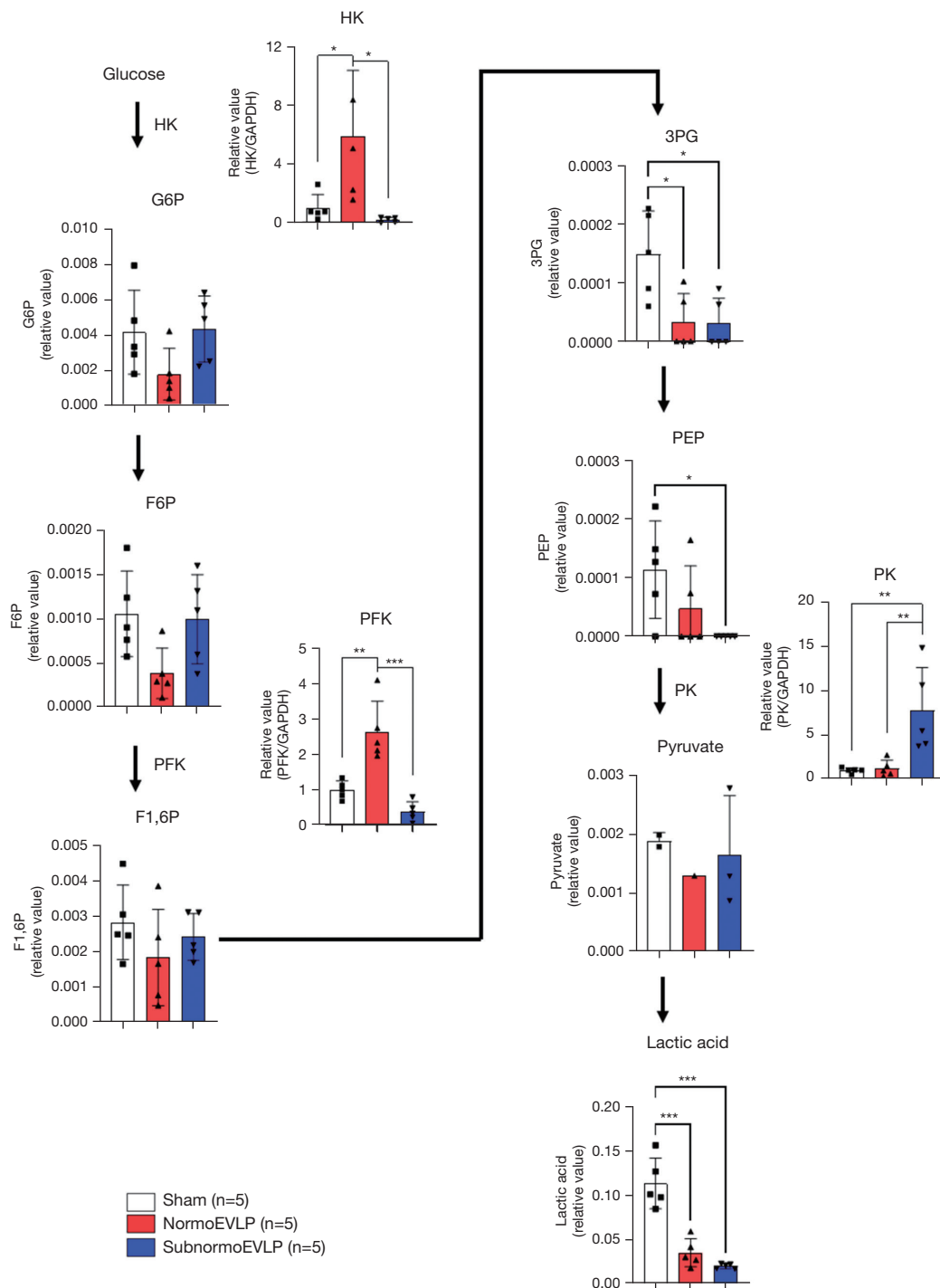
Figure 5 Metabolite levels in glycolysis pathways. The metabolites associated with glucose metabolism (G6P, F6P, F1,6P) tend to be lower in the normoEVLP group than in the subnormoEVLP group. HK and PFK—important enzymes in glycolysis—show significantly higher expression levels in the normoEVLP group than in the subnormoEVLP group (*, P<0.05; **, P<0.01; and ***, P<0.001, one-way analysis of variance). HK, hexokinase; G6P, glucose-6-phosphate; GAPDH, glyceraldehyde 3-phosphate dehydrogenase; F6P, fructose-6-phosphate; PFK, phosphofructokinase; F1,6P, fructose-1,6-bispohsphate; EVLP, ex vivo lung perfusion; 3PG, 3-phosphoglycerate; PEP, phosphoenolpyruvate; PK, pyruvate kinase.
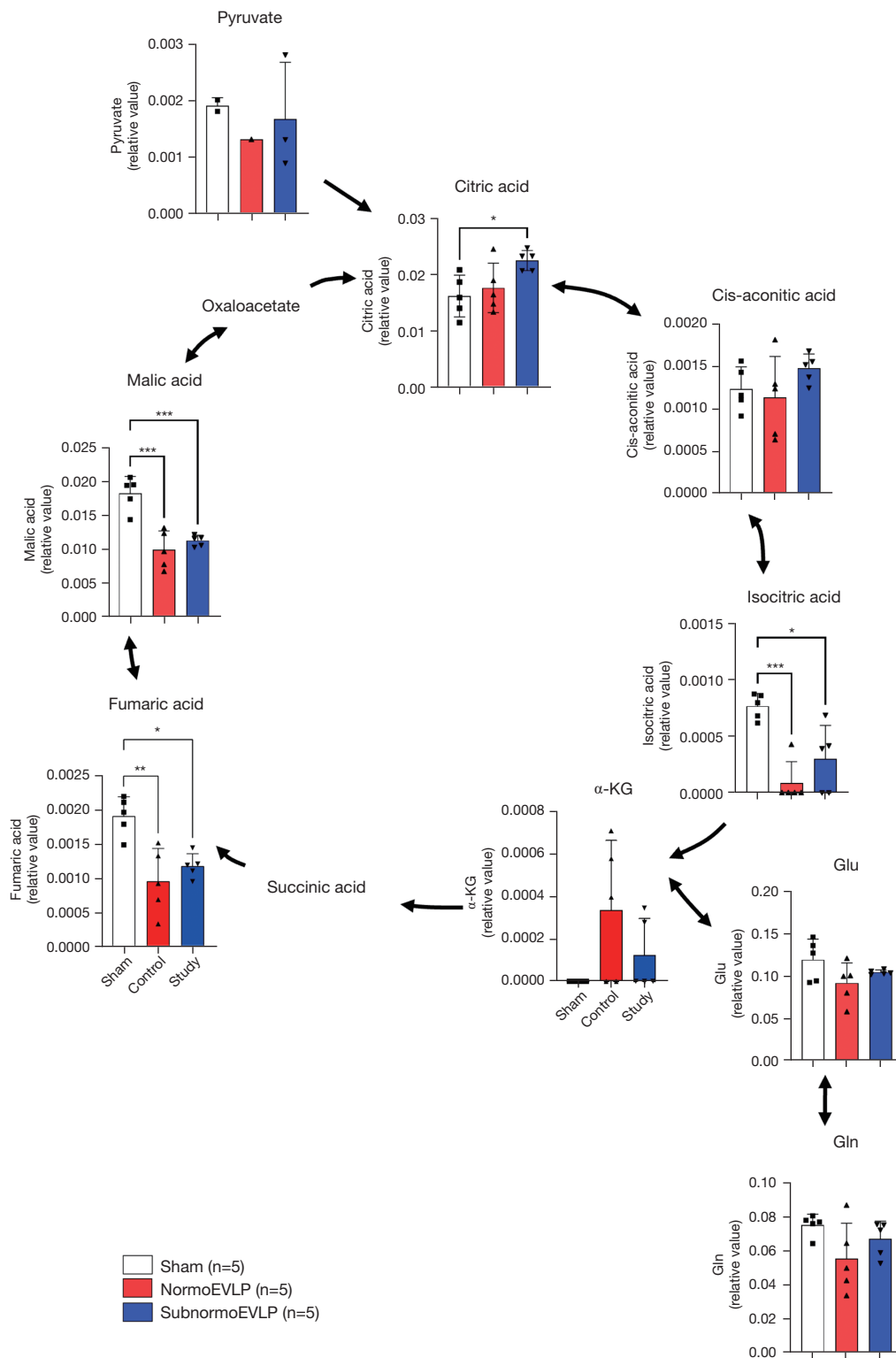
Figure 6 Metabolite levels in the TCA cycle. Isocitric acid, fumaric acid, and malic acid were significantly decreased in EVLP groups compared with sham (*, $P<0.05$; **, $P<0.01$; and ***, $P<0.001$; one-way analysis of variance). α-KG, α-ketoglutarate; Gln, glutamine; Glu, glutamate; EVLP, ex vivo lung perfusion; TCA, tricarboxylic acid.
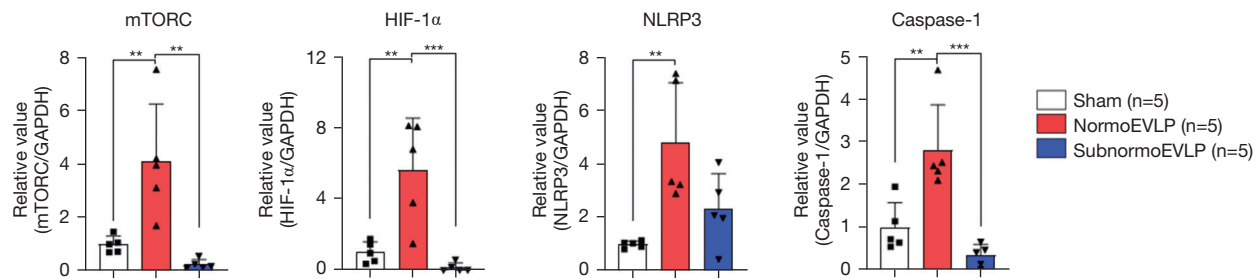
Figure 7 Expression levels of mTORC, HIF-1α, NLRP3, and caspase-1 in samples from the sham, normoEVLP, and subnormoEVLP groups. mTORC, HIF-1α, and caspase-1 expression are significantly increased in the normoEVLP group compared with that in the subnormoEVLP group (**, $P<0.01$ and ***, $P<0.001$, one-way analysis of variance). mTORC, mammalian target of rapamycin complex; GAPDH, glyceraldehyde 3-phosphate dehydrogenase; HIF-1α, hypoxia-inducible factor 1α; NLRP3, nucleotide-binding domain, leucine-rich-containing family pyrin domain containing 3; EVLP, ex vivo lung perfusion.

most favorable for lung preservation remains unclear.

Previous studies on the ideal temperature for organ preservation using machine perfusion have been conducted, particularly subnormothermic or hypothermic machine perfusion (HMP) in kidney and liver transplants. Based on better nutrient supply and endothelial protection (27), HMP is the gold standard for circulatory death kidney transplantation (28). In liver transplantation, HMP stimulates aerobic metabolism while limiting organ metabolism and oxygen demand (27). HMP settings are already in clinical use for kidney (27,29) and liver (30) transplants.

Meanwhile, several recent studies have been conducted on the perfusate temperature in lung transplantation, demonstrating that subnormothermic EVLP can effectively lower the metabolic rate, decrease oxygen demand, and facilitate the removal of metabolic waste products while restoring adenosine triphosphate (ATP) levels (27,29,30). Extreme subnormothermic perfusate temperatures, such as 21 ℃, have disadvantages in terms of PVR and edema. Therefore, moderate subnormothermia is more advantageous than low subnormothermia (8).

In this study, subnormothermic EVLP showed favorable results for OC and PVR compared with normothermic EVLP. The observed changes in inflammatory cytokine levels supported these results. The levels of inflammatory cytokines such as TNF-α, IL-1β, IL-6, and IL-18 were significantly higher in the normothermic EVLP group than in the sham-treated and subnormothermic EVLP groups. Histopathologically, subnormothermic EVLP caused less lung injury than normothermic EVLP according to the LIS scores. In summary, subnormothermic EVLP leads

to superior graft function and causes less graft injury and inflammation than normothermic EVLP. Some recent studies on subnormothermic EVLP have reported similar results. Arni *et al.* showed that EVLPs at 28 ℃ had more protective effects than those at normothermia, with a better physiological state of the donation after circulatory death graft after 4 h of EVLP (8). Physiological data, including PVR, edema, compliance, and OC, significantly improved at low perfusate temperatures, which was due to the improvement of the tissue ATP content and decreased secretion of pro-inflammatory cytokines (8). In another study conducted by the same authors, perfusion at subnormothermia was shown to have strong benefits for both physiological parameters and attenuation of IR injury in a rat model (7).

"Metabolic reprogramming" is an altered configuration of cellular metabolism to meet the specialized needs of cells exposed to stimuli or stressors (31). Previous studies have observed this metabolic reprogramming during IR. In previous studies, IR injury was found to occur when aerobic metabolism changed to anaerobic metabolism due to brief IR (32,33). During ischemia, energy metabolism switches from fatty-acid oxidation to oxidative glycolysis for ATP production (34,35). During reperfusion, both lipid and protein oxidation processes exceed the levels before the ischemic insult (36).

Especially in glucose metabolism, anaerobic glycolysis is less efficient than oxidative phosphorylation, which is the preferred metabolic pathway in highly proliferative cells such as cancer cells and those involved in inflammation, although under aerobic conditions (37-40). During inflammatory responses, immune cells, such as macrophages

and T cells, undergo this metabolic shift (39-41); the inflammatory phase favors anaerobic glycolysis, whereas oxidative phosphorylation dominates the resolution phase of inflammation (37). This metabolic reprogramming in glycolysis promotes the inflammatory response in an animal model of acute lung injury (ALI). In a mouse model of ALI, glycolysis was enhanced during ALI and augmented the inflammatory response (42-44). In another murine model of ALI, the PFK2 enzyme, which is involved in glycolysis, acted as an innate protective mechanism of alveolar epithelial cell metabolism (21), and glycolysis contributed to the profibrotic phenotype in the lung (39). The inflammatory M1 phenotype of macrophages relies on glycolysis, which breaks down in the TCA cycle in chronic lung disease (40).

In our study, changes in the glycolysis pathway were particularly significant. HK and PFK, important enzymes involved in glycolysis, were significantly downregulated in the subnormoEVLP group compared with those in the normoEVLP group, whereas the levels of glycolysis intermediate metabolites tended to be increased in the subnormoEVLP group. This means that intermediate metabolites accumulate due to decreased activity in the glycolysis pathway in subnormoEVLP. Based on these results, we inferred that metabolic reprogramming to the glycolytic process occurred in the normoEVLP group, and the inflammatory response was intensified. Studies in the field of organ preservation have shown similar results. Decreased lactate levels may indicate that aerobic glycolysis decreased in subnormothermic (28 ℃) EVLP and anaerobic glycolysis increased in normothermic (37 ℃) EVLP (7). However, the TCA cycle for aerobic glycolysis showed similar trends in both groups in this study. This result is considered to show similar energy conversions in both groups due to the inflow of acetyl-coenzyme A (CoA) and succinyl-CoA through branched-chain amino acids and β-oxidation in addition to pyruvate.

mTORC1 mainly maintains a cellular balance between anabolism and catabolism in response to environmental stimuli (45,46), and HIF-1α is an important transcription factor for cells to sense and adapt to changes in oxygen levels (47). In ALI, the HIF-1α-PFK2 axis appears to act as an innate protective mechanism for the critical intersection between alveolar epithelial cell metabolism and lung inflammation (21). HIF-1α and its target genes involved in glucose uptake and glycolysis are upregulated in an mTORC1 signaling-dependent manner (38,46,48). Changes in HIF-1α expression and the metabolic shift

to aerobic glycolysis are the causes of macrophage activation (47) and constitute an important pathway related to NLRP3 inflammasome activation (42,43). Overall, previous studies on ALI confirmed that metabolic reprogramming to glycolysis exerts a pro-inflammatory effect through the mTORC1-HIF-1α-NLRP3 inflammasome axis. In our study, the expression levels of mTORC, HIF-1α, NLRP3, and its effector caspase-1 were significantly lower in the normoEVLP group than in the subnormoEVLP group, as were the expression levels of HK and PFK, which are important enzymes of glycolysis.

This study had some limitations. First, the study was designed to assess the function and metabolites of rat lung grafts after EVLP. Therefore, it did not assess graft function after *in vivo* reperfusion. Second, although subnormothermic conditions showed improvements in graft function during EVLP and we found differences in glycolysis and related gene expression between the groups, it was difficult to clarify the detailed mechanism related to the observed effects. Further experiments with knock-out mice or pharmacological inhibitors are warranted, which may further elucidate the relevant pathways.

Conclusions

Our study provided a schematic of the glycolytic pathways in lung IR and identified the effects of perfusate temperature on IR during EVLP. The study results confirm that subnormothermic EVLP led to better graft function than normothermic EVLP. Considering the changes in metabolomics, pro-inflammatory cytokines, and graft function, the protective effects of subnormothermic EVLP might be caused by a metabolic shift to glycolysis. Compared to the subnormothermic EVLP group, the normothermic EVLP group predominantly used glycolysis for energy metabolism. In normothermic EVLP, changes in the glycolytic phenotype occurred through the mTORC1-HIF-1α-NLRP3 pathway, and the ensuing increased secretion of pro-inflammatory cytokines caused deterioration of graft function. These changes were attenuated by subnormal temperature, protecting the graft. Although our study showed somewhat broad and general insight into the perfusate temperature of EVLP, the differences observed in glycolysis activity and the expression levels of mTORC, HIF-1α, and NLRP3 during EVLP suggest that these molecules may act as potential target candidates to induce improvement in lung function. Therefore, further experiments utilizing the inhibition or

activation of these molecules may verify the enhancement of lung function using EVLP.

Footnote

Reporting Checklist: The authors have completed the ARRIVE reporting checklist. Available at https://jtd.amegroups.com/article/view/10.21037/jtd-23-1809/rc

Data Sharing Statement: Available at https://jtd.amegroups.com/article/view/10.21037/jtd-23-1809/dss

Peer Review File: Available at https://jtd.amegroups.com/article/view/10.21037/jtd-23-1809/prf

Conflicts of Interest: All authors have completed the ICMJE uniform disclosure form (available at https://jtd.amegroups.com/article/view/10.21037/jtd-23-1809/coif). The authors have no conflicts of interest to declare.

Ethical Statement: The authors are accountable for all aspects of the work in ensuring that questions related to the accuracy or integrity of any part of the work are appropriately investigated and resolved. All experimental and animal care procedures were conducted in accordance with the Laboratory Animal Welfare Act, the Guide for the Care and Use of Laboratory Animals provided by the Ajou University Institutional Animal Care and Use Committee (IACUC) (No. 2016-0047), and the Guide for the Care and Use of Laboratory Animals (NIH Publication No. 86-23, revised 1996).

References

1. George TJ, Arnaoutakis GJ, Beaty CA, et al. A physiologic and biochemical profile of clinically rejected lungs on a normothermic ex vivo lung perfusion platform. J Surg Res 2013;183:75-83.
2. Sadaria MR, Smith PD, Fullerton DA, et al. Cytokine expression profile in human lungs undergoing normothermic ex-vivo lung perfusion. Ann Thorac Surg 2011;92:478-84.
3. Pan X, Yang J, Fu S, et al. Application of ex vivo lung perfusion (EVLP) in lung transplantation. J Thorac Dis 2018;10:4637-42.
4. Cypel M, Yeung JC, Liu M, et al. Normothermic ex vivo lung perfusion in clinical lung transplantation. N Engl J Med 2011;364:1431-40.
5. Cypel M. Ex vivo lung perfusion (EVLP). Curr Respir Care Rep 2013;2:167-72.
6. Burki S, Noda K, Kumar A, et al. Influence of various perfusion temperatures on lung graft preservation during ex vivo lung perfusion. J Heart Lung Transplant 2019;38:S240-1.
7. Arni S, Maeyashiki T, Citak N, et al. Subnormothermic Ex Vivo Lung Perfusion Temperature Improves Graft Preservation in Lung Transplantation. Cells 2021;10:748.
8. Arni S, Maeyashiki T, Opitz I, et al. Subnormothermic ex vivo lung perfusion attenuates ischemia reperfusion injury from donation after circulatory death donors. PLoS One 2021;16:e0255155.
9. Yeung JC, Zamel R, Klement W, et al. Towards donor lung recovery-gene expression changes during ex vivo lung perfusion of human lungs. Am J Transplant 2018;18:1518-26.
10. Hsin M, Au T. Ex vivo lung perfusion: a potential platform for molecular diagnosis and ex vivo organ repair. J Thorac Dis 2018;10:S1871-83.

11. Dromparis P, Aboelnazar NS, Wagner S, et al. Ex vivo perfusion induces a time- and perfusate-dependent molecular repair response in explanted porcine lungs. Am J Transplant 2019;19:1024-36.

12. Wallinder A, Ricksten SE, Silverborn M, et al. Early results in transplantation of initially rejected donor lungs after ex vivo lung perfusion: a case-control study. Eur J Cardiothorac Surg 2014;45:40-4; discussion 44-5.

13. Sage E, Mussot S, Trebbia G, et al. Lung transplantation from initially rejected donors after ex vivo lung reconditioning: the French experience. Eur J Cardiothorac Surg 2014;46:794-9.

14. Bozso S, Freed D, Nagendran J. Successful transplantation of extended criteria lungs after prolonged ex vivo lung perfusion performed on a portable device. Transpl Int 2015;28:248-50.

15. Zeriouh M, Sabashnikov A, Mohite PN, et al. Utilization of the organ care system for bilateral lung transplantation: preliminary results of a comparative study. Interact Cardiovasc Thorac Surg 2016;23:351-7.

16. Gloria JN, Yerxa J, Kesseli SJ, et al. Subnormothermic ex vivo lung perfusion attenuates graft inflammation in a rat transplant model. J Thorac Cardiovasc Surg 2022;164:e59-70.

17. Wishart DS. Metabolomics: the principles and potential applications to transplantation. Am J Transplant 2005;5:2814-20.

18. Liu Y, Yan S, Ji C, et al. Metabolomic changes and protective effect of (L)-carnitine in rat kidney ischemia/reperfusion injury. Kidney Blood Press Res 2012;35:373-81.

19. Wyss RK, Méndez Carmona N, Arnold M, et al. Hypothermic, oxygenated perfusion (HOPE) provides cardioprotection via succinate oxidation prior to normothermic perfusion in a rat model of donation after circulatory death (DCD). Am J Transplant 2021;21:1003-11.

20. Schlegel A, Muller X, Dutkowski P. Hypothermic Machine Preservation of the Liver: State of the Art. Curr Transplant Rep 2018;5:93-102.

21. Vohwinkel CU, Burns N, Coit E, et al. HIF1A-dependent induction of alveolar epithelial PFKFB3 dampens acute lung injury. JCI Insight 2022;7:e157855.

22. Noda K, Shigemura N, Tanaka Y, et al. Successful prolonged ex vivo lung perfusion for graft preservation in rats. Eur J Cardiothorac Surg 2014;45:e54-60.

23. Haam S, Noda K, Philips BJ, et al. Cyclosporin A Administration During Ex Vivo Lung Perfusion Preserves Lung Grafts in Rat Transplant Model. Transplantation 2020;104:e252-9.

24. Haam S, Lee JG, Paik HC, et al. Hydrogen gas inhalation during ex vivo lung perfusion of donor lungs recovered after cardiac death. J Heart Lung Transplant 2018;37:1271-8.

25. Yamamoto H, Fujimori T, Sato H, et al. Statistical hypothesis testing of factor loading in principal component analysis and its application to metabolite set enrichment analysis. BMC Bioinformatics 2014;15:51.

26. Cypel M, Yeung JC, Hirayama S, et al. Technique for prolonged normothermic ex vivo lung perfusion. J Heart Lung Transplant 2008;27:1319-25.

27. Patel K, Smith TB, Neil DAH, et al. The Effects of Oxygenation on Ex Vivo Kidneys Undergoing Hypothermic Machine Perfusion. Transplantation 2019;103:314-22.

28. Rojas-Pena A, Bartlett RH. Ex Situ Organ Preservation: The Temperature Paradigm. Transplantation 2018;102:554-6.

29. Kataria A, Magoon S, Makkar B, et al. Machine perfusion in kidney transplantation. Curr Opin Organ Transplant 2019;24:378-84.

30. Schlegel A, Dutkowski P. Role of hypothermic machine perfusion in liver transplantation. Transpl Int 2015;28:677-89.

31. Aboushousha R, Elko E, Chia SB, et al. Glutathionylation chemistry promotes interleukin-1 beta-mediated glycolytic reprogramming and pro-inflammatory signaling in lung epithelial cells. FASEB J 2021;35:e21525.

32. Kvietkauskas M, Zitkute V, Leber B, et al. The Role of Metabolomics in Current Concepts of Organ Preservation. Int J Mol Sci 2020;21:6607.

33. Erpicum P, Rowart P, Defraigne JO, et al. What we need to know about lipid-associated injury in case of renal ischemia-reperfusion. Am J Physiol Renal Physiol 2018;315:F1714-9.

34. Buchko MT, Stewart CJ, Hatami S, et al. Total parenteral nutrition in ex vivo lung perfusion: Addressing metabolism improves both inflammation and oxygenation. Am J Transplant 2019;19:3390-7.

35. Eltzschig HK, Eckle T. Ischemia and reperfusion--from mechanism to translation. Nat Med 2011;17:1391-401.

36. Ayene IS, Dodia C, Fisher AB. Role of oxygen in oxidation of lipid and protein during ischemia/reperfusion in isolated perfused rat lung. Arch Biochem Biophys 1992;296:183-9.

37. Soto-Heredero G, Gómez de Las Heras MM, Gabandé-Rodríguez E, et al. Glycolysis - a key player in the inflammatory response. FEBS J 2020;287:3350-69.

38. Magaway C, Kim E, Jacinto E. Targeting mTOR and Metabolism in Cancer: Lessons and Innovations. Cells 2019;8:1584.

39. Zhao H, Dennery PA, Yao H. Metabolic reprogramming in the pathogenesis of chronic lung diseases, including BPD, COPD, and pulmonary fibrosis. Am J Physiol Lung Cell Mol Physiol 2018;314:L544-54.

40. Ogger PP, Byrne AJ. Macrophage metabolic reprogramming during chronic lung disease. Mucosal Immunol 2021;14:282-95.

41. Van den Bossche J, O'Neill LA, Menon D. Macrophage Immunometabolism: Where Are We (Going)? Trends Immunol 2017;38:395-406.

42. Zhong WJ, Yang HH, Guan XX, et al. Inhibition of glycolysis alleviates lipopolysaccharide-induced acute lung injury in a mouse model. J Cell Physiol 2019;234:4641-54.

43. Moon JS, Hisata S, Park MA, et al. mTORC1-Induced HK1-Dependent Glycolysis Regulates NLRP3 Inflammasome Activation. Cell Rep 2015;12:102-15.

44. Gong Y, Lan H, Yu Z, et al. Blockage of glycolysis by targeting PFKFB3 alleviates sepsis-related acute lung injury via suppressing inflammation and apoptosis of alveolar epithelial cells. Biochem Biophys Res Commun 2017;491:522-9.

45. Mao Z, Zhang W. Role of mTOR in Glucose and Lipid Metabolism. Int J Mol Sci 2018;19:2043.

46. Yecies JL, Manning BD. Transcriptional control of cellular metabolism by mTOR signaling. Cancer Res 2011;71:2815-20.

47. McGettrick AF, O'Neill LAJ. The Role of HIF in Immunity and Inflammation. Cell Metab 2020;32:524-36.

48. Düvel K, Yecies JL, Menon S, et al. Activation of a metabolic gene regulatory network downstream of mTOR complex 1. Mol Cell 2010;39:171-83.